JOURNAL OF CATALYSIS 99, 28–38 (1986)

Chlorine Promoters in Selective Ethylene Epoxidation over Ag(111): A Comparison with Ag(110)

CHARLES T. CAMPBELL[1]

Los Alamos National Laboratory, Los Alamos, NM 87545

Received July 8, 1985; revised November 12, 1985

Chlorine promoters are added in the silver-catalyzed oxidation of ethylene (C_2H_4 + 1/2 $O_2 \rightarrow$ C_2H_4O) in order to improve the selectivity for ethylene epoxide production. We have recently (Campbell, C. T., and Paffett, M. T., *Appl. Surf. Sci.* **19,** 28, 1984; Campbell, C. T., and Koel, B. E., *J. Catal.* **92,** 272, 1985) modeled the role of chlorine promoters in this reaction by depositing chlorine adatoms onto the Ag(110) surface in ultrahigh vacuum (UHV) and monitoring the resultant effects on the medium-pressure (~1 atm) kinetics of the epoxidation reaction. This was accomplished with an apparatus that allowed rapid (<20 s) transfer of the model catalyst between the UHV chamber for surface analysis (XPS, AES, LEED, AES) and a high-pressure microreactor for kinetics. That work led to a detailed picture of the role of chlorine promoters in this reaction. This present study is an extension of that work to include the Ag(111) surface, which behaves much differently than Ag(110) in dissociative oxygen adsorption [(a) Campbell, C. T., *Surf. Sci.* **157,** 43, 1985; (b) Campbell, C. T., submitted for publication] but nevertheless displays very similar catalytic behavior for this reaction (Campbell, C. T., *J. Catal.* **94,** 436, 1985). The results indicate that the effects of chlorine addition are very similar on Ag(111) and (110). They can be explained with the same reaction mechanism involving adsorbed oxygen and ethylene. The steady-state atomic oxygen coverage (under catalytic reaction conditions) goes through a large maximum with chlorine coverage on Ag(111), not seen with Ag(110). This is due to the very low reactivity of atomic oxygen on Ag(111) in the presence of chlorine. Evidence is presented that suggests that the standard method of measuring the Ag surface area of supported catalysts via oxygen chemisorption is very unreliable.

I. INTRODUCTION

Ethylene epoxidation is a several billion dollar per year industry, catalyzed with a supported Ag catalyst. It has been the subject of intense practical and fundamental research [(*1–23*) and refs. therein]. In our continuing program to study this reaction (*1–7*), we have demonstrated that the Ag(111) and (110) single-crystal surfaces are excellent kinetic models of high-surface-area, supported Ag catalysts, with virtually identical activation energies and reaction orders with respect to ethylene (P_{Et}) and oxygen (P_{O_2}) pressures. We have also addressed the role of Cs promoters in Ag catalysts by dosing Cs adatoms to the Ag(111) surface (*8*).

In industrial processes, chlorinated hydrocarbons are added in trace quantity to the reactant feed in order to improve catalyst selectivity to ethylene epoxide (also called ethylene oxide). This saves some \$8 × 10^8 per year in ethylene costs that normally would be converted to the thermodynamically preferred side products, CO_2 + H_2O. In model kinetic studies using chlorine adatoms in controlled structures and coverages on the Ag(110) surface (*1, 2*), we have recently addressed the role of these chlorine promoters in the reaction.

Our results are consistent with the following mechanism:

$$C_2H_4 \overset{\text{Fast}}{\rightleftharpoons} C_2H_{4,a} \quad (1)$$

$$O_2 \overset{\text{Fast}}{\rightleftharpoons} O_{2,a} \longrightarrow 2O_a \quad (2)$$

$$C_2H_{4,a} + O_{2,a} \overset{\text{Slow}}{\longrightarrow} I_a \quad (3)$$

[1] Present address: Chemistry Dept., Indiana University, Bloomington, IN 47405.

0021-9517/86 \$3.00

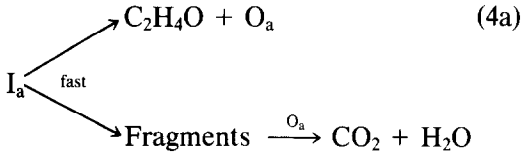

Forms of this mechanism have been proposed previously [(*9–15*) and refs. therein]. The adsorbed intermediate (I_a) is formed in the rate-determining step. The selectivity, however, is determined by the branching ratio of fast steps leading to the decomposition of this intermediate. Chlorine adatoms, deposited by the chlorinated hydrocarbons, have electronic effects on the heats of adsorption of ethylene and molecular O_2, which alter the steady-state coverages of these species under reaction conditions. This gives rise to understandable changes in the rate of the slow step (Step (3) above), which are, however, unrelated to the selectivity. The selectivity is controlled by the chlorine coverage via an ensemble effect on the rapid branching ratio (Step (4) above). Fragmentation of the intermediate (Step (4b)) seems to require larger ensembles of chlorine-free Ag sites than does the epoxidation branch (Step (4a)). Note that this is in contrast to an earlier model (*14*), which attributed the enhancement of selectivity entirely to the effect of chlorine on the dissociation rate of O_2. Such a model is discarded since the latter effect occurs at low θ_{Cl}, while the former effect is only at high θ_{Cl} (*1*).

The present study is an extension of this previous work, where we now investigate the effects of chlorine adatoms on kinetics occurring at Ag(111). In this case, results are quite similar to those for Cl/Ag(110). There are differences that can be understood on the basis of the above mechanism.

II. EXPERIMENTAL

The apparatus and techniques have been explained previously (*3, 4, 6*). In short, the crystal surface was cleaned under ultrahigh vacuum (UHV) and verified with AES, XPS, and LEED. Chlorine adatoms were deposited in controlled quantities as described previously (*1*). The chlorine surface coverage (θ_{Cl}) was taken as proportional to the ratio of Cl(LMM) to Ag(MNN) AES peak-to-peak intensities (I_{Cl}/I_{Ag}): (Modulation = $5V_{p-p}$, retarding ratio = 3, normal detection, 5-kV incident beam.) The sample was translated to an attached batch microreactor, pressurized with the reaction mixture, and heated to reaction temperature until a steady-state (low conversion limit) rate was established. Rates of ethylene epoxide (EtO) and CO_2 production were monitored by product buildup via gas chromatography. After reaction, the sample was translated back into UHV rapidly (<17 s), and the surface was examined by surface spectroscopies. The chlorine coverage and LEED structures did not change significantly during the course of a reaction rate measurement, except when noted below. Thermal desorption spectroscopy was used as described previously (*1, 6*) to measure the steady-state coverage of atomically adsorbed oxygen (O_a) existing on the surface under reaction conditions. Coverages (θ) are defined relative to the number of Ag surface atoms, 1.38×10^{15} cm^{-2} for Ag(111).

III. RESULTS

A. Chlorine Adsorption

The surface structures formed by chlorine adatoms on Ag(111) have been studied by a number of authors (*19–22*). As our methods of chlorine adatom deposition are somewhat different, we performed a few experiments to verify that the same general behavior exists. The AES signal for chlorine nominally saturates at room temperature at an AES ratio $I_{Cl}/I_{Ag} = 0.24 \pm 0.01$. Here and up to about 500 K we observed a LEED pattern identical to that referred to as "pattern C" by Bowker and Waugh (*22*). This has been interpreted as a single layer of AgCl(111) on the surface of Ag(111), with associated coincidence lattice spots (*19, 21, 22*). This model gives a chlorine

coverage $\theta_{Cl}^{sat} = 0.52$, which we use for calibration purposes. This structure gives a Cl/Ag AES ratio very close to that for saturation Cl/Ag(110) ($\theta_{Cl} = 0.75$) under identical measurement conditions (*2*). This has been noted previously (*19*) and related to the similarities in the overlayer structures, where in both cases the topmost layer consists of a nearly hexagonal layer of chlorine atoms (ions).

Upon heating the saturated adlayer, the Cl-AES signal varies as shown in Fig. 1. The increase up to about 650 K is reminiscent of observations by Bowker and Waugh (*22*), and may reflect the existence of some subsurface dissolved chlorine. For consistency in calibration of chlorine coverages, we measured Cl/Ag ratios in the temperature range 300 to 400 K. Above 650 K desorption [as AgCl (*22*)] begins, and is completed by about 800 K.

B. Kinetics of Ethylene Epoxidation

Figure 2 shows the variation in steady-state reaction rates and selectivity with chlorine coverage at 563 K, 150 Torr O_2 and 20 Torr ethylene (Et). The rates are expressed as a turnover frequency (TON_i), i.e., the number of molecules of *i* produced per surface Ag atom (site) per second. We have assumed, as substantiated previously (*4*), 10^{15} surface Ag atoms (sites) on this Ag(111) sample. Also shown is the total rate of ethylene consumption, $TON_{Et} = TON_{EtO} + TON_{CO_2}/2$. The selectivity to ethylene oxide with respect to ethylene conversion is defined as $S_{EtO} = TON_{EtO}/TON_{Et}$.

Figure 3 shows the variation in steady-state reaction rates and selectivity at 490 K, 150 Torr O_2 and 4.1 Torr Et. The results of Figs. 2 and 3 for Ag(111) are qualitatively very similar to those previously presented

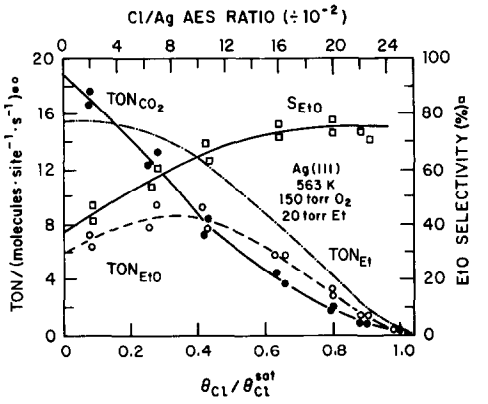

FIG. 2. Variation in the steady-state reaction rates and selectivity with chlorine coverage on Ag(111) at 563 K, 20 Torr Et, and 150 Torr O_2.

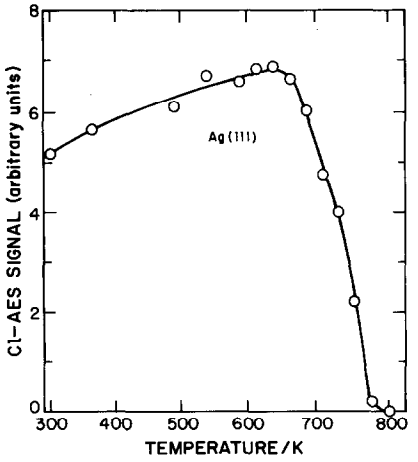

FIG. 1. Variation of the Cl-AES peak-to-peak height with increasing temperature for an initially saturated Cl overlayer on Ag(111) that is heated under vacuum.

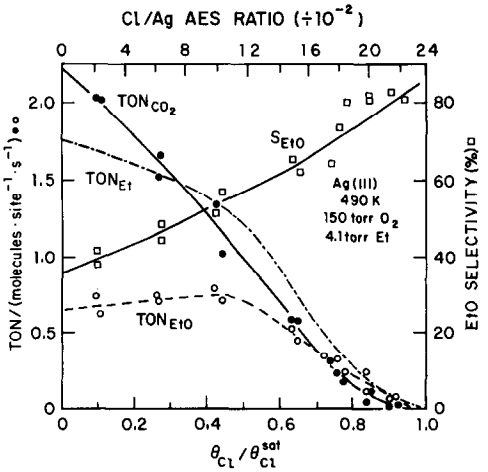

FIG. 3. Variation in the steady-state reaction rates and selectivity with chlorine coverage on Ag(111) at 490 K, 4.1 Torr Et, and 150 Torr O_2.

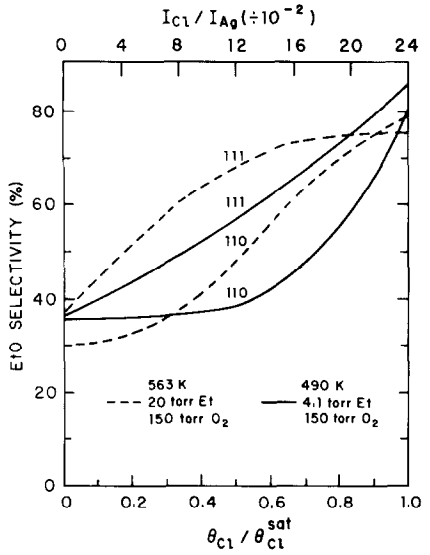

FIG. 4. Data of Figs. 2 and 3 replotted to show only the selectivity variations on Ag(111) with chlorine coverage. For comparison, data under the same conditions on Ag(110) from (*1*, *2*) are shown. The data for Ag(110) from (*1*) have been corrected slightly due to an error in gas-chromatograph sensitivity calibration discussed previously (*4*).

(*1*, *2*) under identical conditions for Ag(110), provided the chlorine coverages are scaled to the saturation values (θ_{Cl}^{sat}) on either surface. A notable difference is displayed in Fig. 4, where the selectivity variations are compared for these two surfaces. It is clear that the selectivity begins to improve at a markedly lower relative chlorine coverage on Ag(111). Note in Figs. 2 and 3 that, similar to Ag(110) (*1*, *2*), there is *no* simple linear falloff in the rate of ethylene consumption with θ_{Cl}. Thus, much more complex kinetic effects are involved than a simple site-blocking of Step (3) in the mechanism, as was pointed out in (*2*).

As noted previously (*1*, *6*), we are able to maintain the steady-steady coverage of atomically adsorbed oxygen existing on the surface under reaction conditions by rapid (~17 s) transfer back into UHV. This coverage is quantified using the ~580 K O_2-TDS peak area or the O(KVV) AES peak-to-peak height (*1*, *6*). The results for the oxygen coverage (θ_O) obtained for the conditions of Fig. 3 are presented in Fig. 5, where they are also compared with data under identical conditions on Ag(110). Oxygen coverages are in absolute units for either surface. The rapid decrease in θ_O with θ_{Cl} on Ag(110) is a direct reflection of the effect of chlorine upon the dissociative sticking probability for O_2 (*1*). Although it appears that chlorine on Ag(111) has a similar strongly negative influence on the dissociative sticking probability for O_2 (see below), the effect is not so directly reflected in the steady-state oxygen adatom coverage under epoxidation reaction conditions. Up to ~30% of saturation, a similar effect seems to appear. However, when θ_{Cl} exceeds 0.3 θ_{Cl}^{sat}, the oxygen coverage begins to grow rapidly, reaches a maximum at about 0.5 θ_{Cl}^{sat}, and then declines near saturation.

The data of Fig. 5 were obtained by O_2-TDS (at ~580 K), but were confirmed by AES intensities. The O(KVV) peak here showed essentially identical lineshape as that for the $p(4 \times 4)$ structure of atomic oxygen on clean Ag(111) (*3*). The O(1*s*)

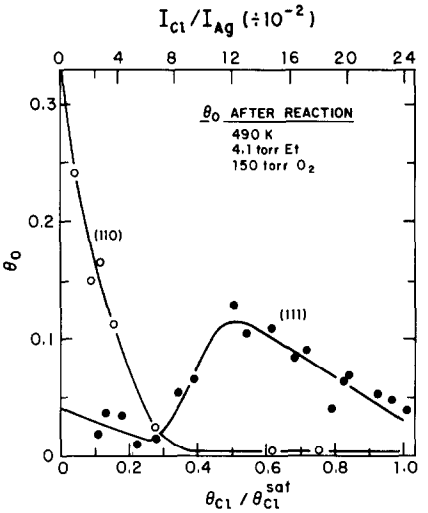

FIG. 5. Variation in the steady-state coverage of atomically adsorbed oxygen (θ_O) with chlorine coverage for the kinetic data on Ag(111) of Fig. 3: 490 K, 4.1 Torr Et, and 150 Torr O_2. Shown for comparison are data under identical conditions on Ag(110) from (*1*).

peak in XPS after reaction for $\theta_{Cl} = 0.55\ \theta_{Cl}^{sat}$ was very similar to that for the $p(4 \times 4)$ structure (*3*) as well, shifted only slightly to high binding energy perhaps due to Cl–O interactions.

Postreaction LEED analysis further confirmed the nature of the oxygen existing under reaction conditions. A $p(4 \times 4)$ pattern was observed after reaction for chlorine coverages between 0.3 θ_{Cl}^{sat} and 0.7 θ_{Cl}^{sat}, as shown in Fig. 6. This is the same pattern as for saturation O_a coverage on clean Ag(111). For $\theta_{Cl} > 0.8\ \theta_{Cl}^{sat}$, complex LEED patterns were seen that will not be discussed. Although these data support a structure for the oxygen quite similar to that for the $p(4 \times 4)$-O structure of clean Ag(111), its reactivity for titration with CO was markedly reduced due to the presence of chlorine (see below).

The data of Fig. 5 for Ag(111) were reproduced at 514 K (same pressures) by O_2-TDS and O-AES. The results were virtually the same at 514 K as at 490 K, with a somewhat higher maximum θ_O, reached at slightly lower θ_{Cl}.

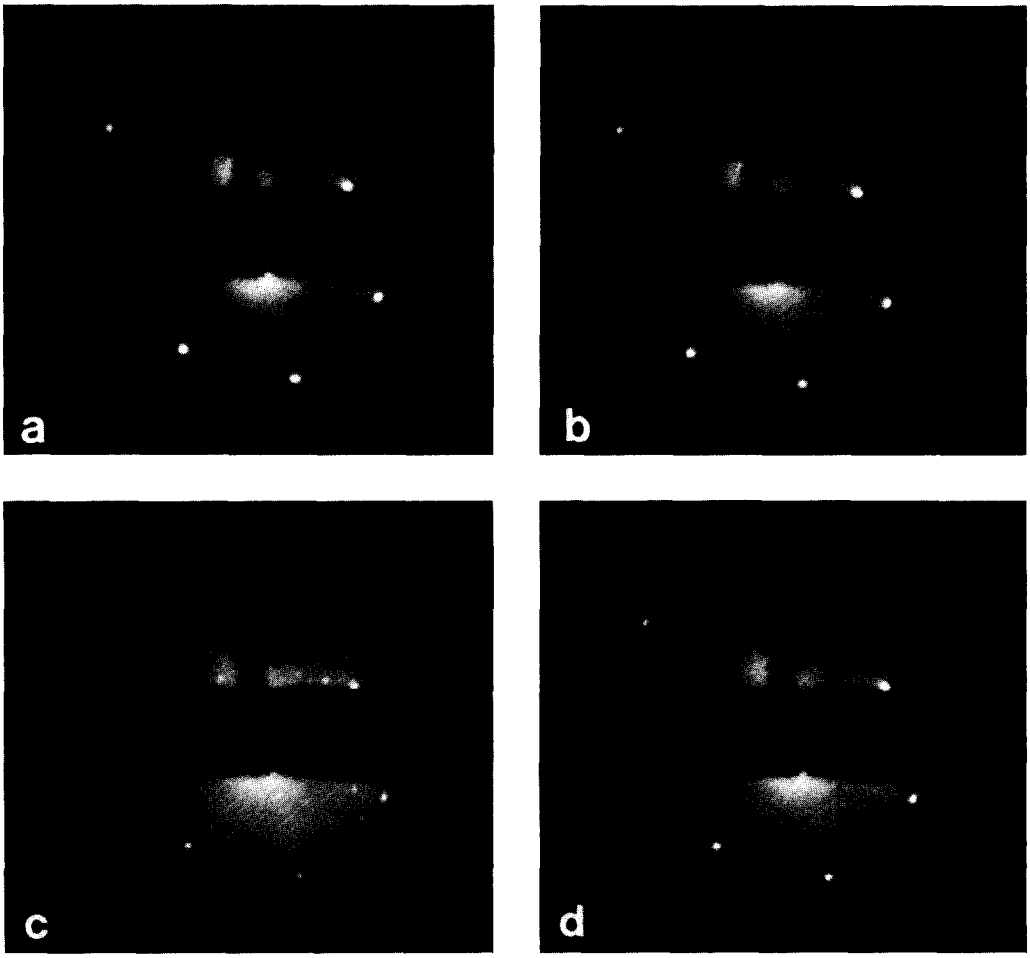

FIG. 6. Low-energy electron diffraction patterns at room temperature for Ag(111) with an incident electron beam of 104 eV about 4° off normal. (a) Clean Ag(111). (b) For $\theta_{Cl} = 0.18\ \theta_{Cl}^{sat}$, after steady-state reaction at 490 K, 4.1 Torr Et, and 150 Torr O_2 for comparison with Figs. 3–5. (c) For $\theta_{Cl} = 0.53\ \theta_{Cl}^{sat}$, after steady-state reaction as in (b). Note the distinct $p(4 \times 4)$-O features that have developed. (d) Same as (c), only after flashing to 660 K to desorb the oxygen. The increased background over clean Ag(111) is due to the disordered chlorine overlayer still remaining on the surface.

C. Coadsorption of Chlorine and Oxygen

The effect of preadsorbed chlorine upon the dissociative adsorption of O_2 on Ag(111) is shown in Fig. 7. Shown here is the oxygen adatom coverage (O_2-TDS peak area) obtained by a 20-s dose at 490 K for various O_2 pressures. Absolute oxygen coverages are calibrated with respect to the $p(4 \times 4)$-O structure of clean Ag(111) (*3*). For comparison, we show also the results for Ag(110) at 50 Torr O_2 from (*2*). Chlorine coverages above θ_{Cl}^{sat} were obtained by room-temperature Cl_2 exposures well above that required for nominal saturation. Such doses lead to substantial incorporation of chlorine into the bulk of the Ag (*22*). One can see in Fig. 7 that, when very large exposures of O_2 are dosed at 490 K, Cl_a does not greatly influence the oxygen adsorption capacity of the Ag surfaces until the chlorine monolayer is completed. The

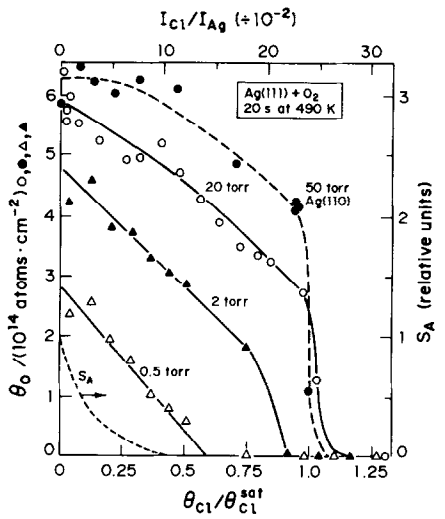

FIG. 7. Variation with chlorine coverage of the amount of adsorbed oxygen accumulated with a 20-s O_2 dose at 490 K and various O_2 pressures on Ag(111). Shown also are data from (*2*) for Ag(110) at 50 Torr O_2. Note that these high-pressure O_2 doses are typical of procedures used to measure the clean Ag surface area of supported Ag catalysts via oxygen chemisorption. For comparison with the lower pressure data, we show the variation in the low-coverage, dissociative O_2 sticking probability (S_A) with chlorine coverage on Ag(110) from (*1*).

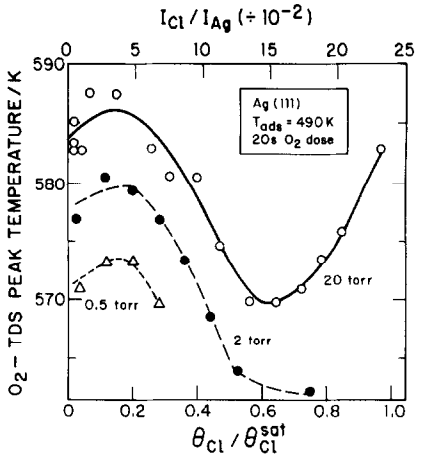

FIG. 8. Variation in oxygen thermal desorption peak temperature with chlorine coverage for the same data used to construct Fig. 7. β = 15 K/s. Oxygen coverages can be taken from Fig. 7.

chlorine-saturated surface will not adsorb O_2 at these exposures. As the exposure decreases, the influence of chlorine becomes much more marked. At 10 Torr · s, we are beginning to see the influence of θ_{Cl} upon the dissociative sticking probability for O_2 on Ag(111). On Ag(110), this has been measured directly (*1*) and is shown here for comparison. It decreases almost exponentially to zero at $\theta_{Cl} \cong 0.4\ \theta_{Cl}^{sat}$. We should note that a $p(4 \times 4)$ LEED pattern, characteristic of O_a on Ag(111), was seen for the 20-Torr dose at $\theta_{Cl} = 0.35\ \theta_{Cl}^{sat}$. Other chlorine coverages were not tested, but we expect that the $p(4 \times 4)$ structure exists after oxygen dosing for a range of chlorine coverages based on the observations after reaction (Fig. 6).

In Fig. 8 we summarize the effects of chlorine upon the O_2-TDS peak temperature for the data used in Fig. 7. The behavior is complex. A major feature is the 15 K decrease in peak temperature up to about 65% of saturation. This far exceeds the ~5 K decrease expected from the accompanying decrease in θ_O. (The coverage can be obtained from Fig. 7, and the resulting temperature decrease at $\theta_{Cl} = 0$ can be seen in Fig. 8). This is similar to data on Ag(110) (*2*). It can be interpreted as a repulsive in-

teraction between O_a and Cl_a, leading to a decreased heat of adsorption for the oxygen adatoms. A first-order Redhead analysis of these peak temperatures, such as used for the clean surface (*3*), would indicate a decrease by 1.1 kcal mole^{-1} in the heat of adsorption of O_2. Above 65% of saturation the effect reverses: a marked increase in the desorption temperature is seen. This was accompanied by a large increase in width of the O_2-TDS peak from ~23 K FWHM below 0.65 θ_{Cl}^{sat} to ~42 K at higher θ_{Cl}. One possible explanation for this behavior is that below 0.65 θ_{Cl}^{sat}, oxygen desorption is rate-limited by actual associative desorption; and, above 0.65 θ_{Cl}^{sat}, oxygen desorption is rate-limited by diffusion of oxygen atoms out of the subsurface region and onto the surface. This temperature difference is consistent with isotopic labeling experiments that probed the nature of subsurface dissolved oxygen on Ag(110) (*23*).

Figure 9 summarizes the results of experiments that compare the reactivity with CO of adsorbed atomic oxygen in the presence and absence of coadsorbed chlorine. Here we show the time evolution of CO_2 product when adsorbed atomic oxygen is exposed at room temperature to a stepwise increase in CO partial pressure (from ~0 to 3×10^{-6} Torr). The CO_2 mass spectrometer signal above background is proportional to the rate of the reaction:[1] $CO + O_a \rightarrow CO_2$. The results for the $p(4 \times 4)$-O overlayer on clean Ag(111) are reproduced from (*3*). For the case of coadsorption with chlorine, the chlorine was first adsorbed, then oxygen was deposited at 20 Torr O_2 pressure for 20 s at 490 K, exactly as in Figs. 7 and 8. Note that this generally gave a $p(4 \times 4)$ LEED pattern (see above). The results of Fig. 9 were essentially the same for the range of chlorine coverages tested: 60 to 75% of saturation. They show that atomic oxygen coadsorbed with chlorine is much less reactive with CO than atomic oxygen on clean

[1] Here we assume that the angular distribution of CO_2 evolution is independent of θ_0 and θ_{Cl}.

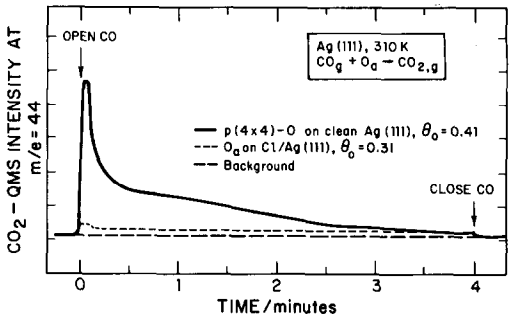

FIG. 9. Comparison of CO titration kinetics for O_a on Ag(111) in the presence and absence of coadsorbed chlorine. Here we plot the CO_2 signal appearing at the mass spectrometer versus time. At time zero, the CO value is opened to give a stepwise increase in CO partial pressure to 3×10^{-6} Torr. The preadsorbed oxygen is titrated off via the reaction: $CO_g + O_a \rightarrow CO_{2,g}$. The clean results are for a $p(4 \times 4)$-O overlayer (*3*). The Cl/Ag(111) results are characteristic of oxygen deposited with 20 Torr O_2 at 490 K as in Fig. 7, for θ_{Cl} = 60 to 75% of saturation. As seen in Fig. 7, this gives an oxygen predosed coverage of about 75% of the $p(4 \times 4)$ coverage. Note, however, that its reactivity is some 10 times slower.

Ag(111). Furthermore, we observed that the "untitratable" oxygen, appearing as O_2 at ~600 K in thermal desorption after completion of the titration, was roughly twice the quantity of that for oxygen on clean Ag(111). This "untitratable oxygen" is thought to be due to subsurface dissolved oxygen (*3*). We note that it appeared some 6 to 11 K higher in temperature in the subsequent TDS than if the entire oxygen coverage were desorbed (without titration).

IV. DISCUSSION

The general effects of chlorine adatom addition to Ag(111) upon the kinetics and selectivity of ethylene epoxidation are quite similar to those we have observed for Ag(110) (*1*, *2*). We therefore refer the reader to the general model for these effects presented previously (*2*), and summarized in the Introduction. The major effect of chlorine to increase the selectivity clearly occurs *after* the rate-determining step, which involves the formation of an intermediate common to both ethylene epoxide and CO_2 production (Step (3)). This was most

clearly demonstrated by observing that the reaction orders with respect to ethylene and O_2 pressure and the apparent activation energies (which probe only the slow, rate-limiting step) varied with θ_{Cl} in identical fashion for both EtO and CO_2 production (*2*). It is thus the subsequent rapid branching ratio of this intermediate (Step (4)) which is influenced by chlorine to improve selectivity. We have maintained that this occurs mainly via an ensemble effect, since the changes in selectivity occur only at rather high chlorine coverages. This is to be differentiated from electronic effects, which should be complete by $\theta_{Cl} = 1/2\ \theta_{Cl}^{sat}$. The charge transfer from chlorine to silver should have nearly reached its full extent already by this coverage, since dipole repulsions lead to strong depolarization of the Ag–Cl bond at higher coverage. (This depolarization was seen directly in the very nonlinear work function increase with θ_{Cl} on Ag(111) (*20*).)

Some readers may have trouble understanding how different ensemble, or site-size, requirements for Steps (4a) and (4b) result in an increase in selectivity when adding chlorine but are *not* evidenced when comparing the different clean crystal planes. (Note that clean Ag(111), (110), and (100) have very similar selectivities (*4*).) Certainly different ensemble *shapes* are available on these different surfaces. However, if the required ensembles are small (~3 Ag atoms) and not particularly sensitive to the exact geometry of the Ag atom group, the different clean crystal planes will show no difference in selectivity. Small ensembles are also consistent with the high chlorine coverages required to influence selectivity. Note that there *is* a difference between crystal planes with respect to chlorine's influence on selectivity (Fig. 4).

Two major differences between Ag(111) and Ag(110) are observed here and must be discussed and rationalized on the basis of the above model. First, the selectivity begins to increase at considerably lower relative chlorine coverages on Ag(111) than on Ag(110) (Fig. 4). Second, the steady-state O_a coverage under reaction conditions goes through a maximum at ~50% of chlorine saturation on Ag(111), in contrast to Ag(110) where the θ_O was tiny by that chlorine coverage (Fig. 5).

Let us deal with this latter point first. In the case of Ag(110), the rapid decline in θ_O with chlorine coverage was easily understandable. It almost perfectly reflected the effect of chlorine upon the dissociative sticking probability for O_2 (*1*). Figure 7 indicates that chlorine should have a similar effect on the dissociative sticking probability for O_2 on Ag(111) as well. (We note that chlorine has this same effect on Ag powder (*24*) and supported Ag samples (*14*).) This effect is, nevertheless, *not* reflected in the steady-state oxygen coverage under epoxidation conditions on Ag(111) (see Fig. 5). According to our mechanism presented in the Introduction, the major mode of oxygen adatom production for selectivities below 75% is via O_2 dissociative adsorption. At a selectivity of 50%, five times more O_a is produced via O_2 adsorption than via Step (4a) of the mechanism: $I_a \rightarrow EtO + O_a$. Thus, the approach to a maximum for θ_O in Fig. 5 represents the following situation. The rate of formation of O_a is decreasing with θ_{Cl} faster than its rate of consumption (via $CO_2 + H_2O$ production in our mechanism). (This can be seen by comparing data for $P_{O_2} \leq 0.5$ Torr in Fig. 7 with that for TON_{CO_2} in Fig. 3.) This can only be understood if the rate constants for reactions leading to O_a consumption have decreased due to the presence of Cl_a. Such an effect might actually be expected based on the titration results of Fig. 9, where the reactivity of O_a with CO in CO_2 production is markedly lower in the presence of coadsorbed chlorine on Ag(111). If this explanation of Fig. 5 is correct, a similar decrease in reactivity of O_a due to Cl_a should *not* be seen on Ag(110). This must await future experiments.

The similarity in the chlorine coverages at which changes occur in Figs. 5 and 8 is

striking. Maxima in the steady-state oxygen coverage under reaction conditions occur where minima in the desorption peak temperature (or heat of adsorption) occur, and vice versa. The latter tell us something about the mode of bonding of oxygen adatoms, which should also be reflected in their reactivity. According to our mechanism, this reactivity will determine the steady-state O_a coverage. Thus, this similarity in Figs. 5 and 8 is not entirely unexpected.

Given that the oxygen adatom coverage behaves as in Fig. 5, it is not too difficult to understand why significantly lower chlorine coverages are required on Ag(111) to give the same selectivity increase (see Fig. 4). According to our model, the selectivity increases because chlorine blocks sites for Step (4b) in the mechanism, the fragmentation of the intermediate I_a. In our model, Step (4b) requires a larger ensemble of free silver sites than does Step (4a), giving rise to the selectivity increase as chlorine titrates these ensembles. If oxygen adatoms can block these sites in a similar fashion to chlorine adatoms, then one should instead sum the chlorine and oxygen coverages when comparing the selectivities on Ag(111) and (110) in Fig. 4. When examined in this light, the selectivity differences between these silver planes are not large. Although the oxygen coverage jumps up rather abruptly in Fig. 5 on Ag(111), the selectivity increases only gradually (Fig. 3). This, however, is expected in our model since the selectivity is still increasing only weakly with θ_{Cl} ($+\theta_O$) in this low coverage range (see Ag(110) data of Fig. 4). Since the explanation for chlorine enhancement in selectivity is based on an ensemble model, differences between these two surface planes might also be naturally expected.

We mentioned that, in the presence of adsorbed chlorine coverages on the order of 30 to 70% of saturation, atomically adsorbed oxygen forms a $p(4 \times 4)$ LEED pattern. A $p(4 \times 4)$ LEED pattern is characteristic of saturation atomic oxygen on clean Ag(111) (*3*). This might indicate that the oxygen and chlorine segregate into separate island phases on the surface. In such a model, it would be difficult to understand the large reactivity difference between the same oxygen structures in the absence or presence of chlorine, unless reaction occurs mainly at the edges of the oxygen islands. There is indeed evidence to this effect (*3a, 6*). Another possibility is that the oxygen and chlorine form a coadsorbed phase that happens to also have a $p(4 \times 4)$ structure. Adsorbed chlorine might, for example, be in a disordered overlayer on top of the normal $p(4 \times 4)$-O structure. One model for this structure, which has a coverage $\theta_O \cong 0.41$, is that it consists of a single trilayer of $Ag_2O(111)$ (*3*). In this model, half the oxygen resides in the topmost surface layer, while half resides below the first Ag layer. The adsorbed chlorine might, for example, replace the topmost oxygen layer.

Chlorine seems to increase the amount of subsurface oxygen. This is suggested by the increase in O_2 desorption temperature and TDS peak width for high chlorine levels (Fig. 8). It is also suggested by the increased amount of "untitratable" oxygen.

One important point should be made concerning the data of Fig. 7. The Ag surface area of high-surface-area silver catalysts is typically measured by oxygen chemisorption at 480 K and ~20 Torr O_2 (*25–28*). Note in Fig. 7 that, under these high-exposure conditions, the oxygen adsorption capacity of Ag is only slightly decreased by $\theta_{Cl} = 0.95\ \theta_{Cl}^{sat}$. This is to be contrasted with the epoxidation rate, which is almost completely attenuated at these same chlorine levels (Figs. 2 and 3), and Refs. (*1, 2*)). That is, the technique for Ag surface area determination based on oxygen chemisorption is entirely *insensitive* to the presence of impurities (in this case Cl_a) which are sufficiently abundant to decrease the epoxidation rate by more than a factor of 10. This problem may help to explain the very large specific catalytic activity (per surface Ag atom) seen for clean Ag(110) and (111) as compared to the low apparent values re-

ported for high-surface-area Ag catalysts (*4, 5*). That is, the apparently low activity of high-area catalysts may well be due to an overestimate in the active Ag surface area.

We should mention that the mechanism we have used here is by no means universally accepted (*9–12, 18, 29–33*). In particular, one school of thought maintains that ethylene epoxide is produced from adsorbed atomic oxygen (*18, 29–33*). Our reasons for preferring the molecular $O_{2,a}$ mechanism are summarized in Ref. (*4*). Those reasons cannot be ignored in any proposed mechanism. They seem to rule out the low coverage form of atomically adsorbed oxygen ($\theta_O < 0.4$) in the rate-determining step for epoxidation. The rates appear to track more closely the coverage of molecularly chemisorbed O_2 (extrapolated from TDS experiments) (*4*).

Very recent X-ray photoelectron spectroscopic data from our lab (*3b*) indicate a significantly different chemical nature between the molecularly chemisorbed oxygen species on Ag(111) compared to Ag(110). It thus seems unlikely that these very different species could both be making bonds to ethylene on the surface in an identical mechanism with similar kinetics, as we have proposed here. An alternate mechanism should also be considered. It is possible that the molecularly chemisorbed oxygen species act to create a special, high-coverage state of atomically adsorbed oxygen, and that this special state is the true oxidant of ethylene. The kinetic data (*4*) still require, however, that this special state of atomic oxygen has a population which tracts closely the coverage of the molecular chemisorbed species but not that of the lower coverage states of O_a, which are abservable after reaction. This situation would occur whenever the lifetime of this special state was very short, due either to rapid removal by reaction or desorption or by conversion to other adsorbed oxygen species.

Such a model would be consistent with very recent beautiful isotope labeling experiments of van Santen and de Groot, who show that very high coverages of preadsorbed atomic oxygen on Ag powder ($0.5 < \theta_O < 1.0$) can be converted with reasonable selectivity to ethylene epoxide, and that the selectivity increases with molecular oxygen pressure and with atomic oxygen coverage (*33*). A very large increase in reactivity toward CO oxidation has already been demonstrated when θ_O exceeds 0.5 on Ag(110), where the $c(6 \times 2)$ state begins to appear (*34*).

Certainly more experiments will be required before reaching a definite determination of the actual oxygen species forming a bond to ethylene on the surface in this reaction. Several features, however, are already clear. (1) This bond formation is rate-determining under most conditions. (2) This bond formation produces an intermediate, which can rapidly branch into either ethylene epoxide or $CO_2 + H_2O$. (3) Selectivity is largely determined by that branching ratio at low conversions. (4) Chlorine improves the selectivity by altering that branching ratio to favor ethylene epoxide. (5) The chlorine coverage over which this occurs is quite high, suggesting an ensemble rather than electronic explanation.

V. CONCLUSIONS

Chlorine adatom addition to Ag(111) has very similar effects as those on Ag(110) with respect to oxygen chemisorption and the kinetics and selectivity of catalytic epoxidation. The results can be explained by a mechanism where adsorbed oxygen and adsorbed ethylene combine in the rate-determining step to form an adsorbed intermediate, which then rapidly decomposes into ethylene epoxide or into fragments that are further oxidized to produce CO_2 and water. Chlorine addition decreases the probability of this later fragmentation process by blocking necessary vacant Ag sites, resulting in improved selectivity. On Ag(110), the steady-state coverage of O_a under reaction conditions decreased rapidly to very low values upon chlorine addition, reflecting

the effect of Cl_a upon the dissociative O_2 sticking probability. In contrast, on Ag(111) the coverage of O_a goes through a maximum at about half the saturation chlorine coverage, reflecting the very low reactivity of O_a when coadsorbed with chlorine on Ag(111). The standard method of measuring the silver surface area of supported Ag catalysts is via oxygen chemisorption at 480 K and ~50 Torr O_2. We see that this is extremely *insensitive* to the presence of large coverages of adsorbed impurities such as chlorine, and can lead to gross overestimates of the clean Ag surface area available for catalytic reaction.

ACKNOWLEDGMENTS

The author would like to acknowledge the valuable technical assistance of Johnny Anderson in this work, and the loaning of equipment by J. M. White.

REFERENCES

1. Campbell, C. T., and Paffett, M. T., *Appl. Surf. Sci.* **19,** 28 (1984).
2. Campbell, C. T., and Koel, B. E., *J. Catal.* **92,** 272 (1985).
3. (a) Campbell, C. T., *Surf. Sci.* **157,** 43 (1985); (b) Campbell, C. T., submitted for publication.
4. Campbell, C. T., *J. Catal.* **94,** 436 (1985).
5. Campbell, C. T., *J. Vac. Sci. Technol. A* **2,** 1024 (1984).
6. Campbell, C. T., and Paffett, M. T., *Surf. Sci.* **139,** 396 (1984).
7. Campbell, C. T., *in* "ACS Symp. Series No. 288: The New Surface Science in Catalysis," held August 1984 in Philadelphia, p. 210.
8. Campbell, C. T., *J. Phys. Chem.* **89,** 5789 (1985).
9. Voge, H. H., and Adams, C. R., "Advances in Catalysis," Vol. 17, p. 151. Academic Press, New York, 1967.
10. Verykios, X. E., Stein, F. P., and Coughlin, R. W., *Catal. Rev.-Sci. Eng.* **22,** 197 (1980).
11. Sachtler, W. M. H., Backx, C., and van Santen, R. A., *Catal. Rev.-Sci. Eng.* **23,** 127 (1981).
12. Kilty, P. A., and Sachtler, W. M. H., *Catal. Rev.-Sci. Eng.* **10,** 1 (1974).
13. van Santen, R. A., Moolhuysen, J., and Sachtler, W. M. H., *J. Catal.* **65,** 478 (1980).
14. Kilty, P. A., Rol, N. C., and Sachtler, W. M. H., *in* "Proceedings, 5th International Congress on Catalysis, Palm Beach, 1972" (J. W. Hightower, Ed.), Vol. 2, p. 929. North-Holland, Amsterdam, 1973.
15. Cant, N. W., and Hall, W. K., *J. Catal.* **52,** 81 (1978).
16. Force, E. L., and Bell, A. T., *J. Catal.* **40,** 356 (1975).
17. Stoukides, M., and Vayenas, C. G., *J. Catal.* **70,** 137 (1981).
18. Grant, R. B., and Lambert, R. M., *J. Catal.* **92,** 364 (1985).
19. Rovida, G., and Pratesi, F., *Surf. Sci.* **51,** 270 (1975).
20. Goddard, P. J., and Lambert, R. M., *Surf. Sci.* **67,** 180 (1977).
21. Tu, Y.-Y., and Blakely, J. M., *J. Vac. Sci. Technol.* **15,** 563 (1978); *Surf. Sci.* **85,** 276 (1979).
22. Bowker, M., and Waugh, K. C., *Surf. Sci.* **134,** 639 (1983).
23. Backx, C., de Groot, C. P. M., and Biolen, P., *Surf. Sci.* **104,** 300 (1981).
24. Meisenheimer, R. G., and Wilson, J. N., *J. Catal.* **1,** 151 (1962).
25. Harriott, P., *J. Catal.* **21,** 56 (1971).
26. Kanoh, H., Nishimura, T., and Ayame, A., *J. Catal.* **57,** 372 (1979).
27. Verykios, X. E., Stein, F. P., and Coughlin, R. W., *J. Catal.* **66,** 147, 368 (1980).
28. Jarjoui, M., Gavelle, P. C., and Teichner, S. J., *J. Chim. Phys.* **75,** 1069 (1978).
29. Backx, C., Moolhuysen, J., Geenen, P., and van Santen, R. A., *J. Catal.* **72,** 364 (1981).
30. Grant, R. B., and Lambert, R. M., *J. Chem. Soc., Chem. Commun.*, 662 (1983).
31. Grant, R. B., and Lambert, R. M., *in* "Catalysis on the Energy Scene" (S. Kaliaguine and A. Mahay, Eds.), p. 251. Elsevier, Amsterdam, 1984.
32. Grant, R. B., and Lambert, R. M., *Langmuir* **1,** 29 (1985).
33. van Santen, R. A., and de Groot, C. P. M., submitted for publication.
34. Campbell, C. T., and Paffett, M. T., *Surf. Sci.* **143,** 517 (1984).